MOL 15685

DNA STRUCTURAL SIMILARITY IN THE 2:1 COMPLEXES OF THE ANTITUMOR DRUGS YONDELIS™ (TRABECTEDIN) AND CHROMOMYCIN A_3 WITH AN OLIGONUCLEOTIDE SEQUENCE CONTAINING TWO ADJACENT TGG BINDING SITES ON OPPOSING STRANDS

Esther Marco and Federico Gago

Departamento de Farmacología, Universidad de Alcalá, E-28871 Alcalá de Henares, Madrid, Spain

Molecular Pharmacology Fast Forward. Published on September 8, 2005 as DOI: 10.1124/mol.105.015685
This article has not been copyedited and formatted. The final version may differ from this version.

Running title: *Similarities in trabectedin- and chromomycinA_3-DNA complexes*

Address correspondence to: Departamento de Farmacología, Universidad de Alcalá, E-28871 Alcalá de Henares, Madrid, Spain
Telephone: +34 - 918 854 514; Fax: +34 - 918 854 591
e-mail: federico.gago@uah.es

Number of text pages: 19
Number of tables: 5
Number of Figures: 4
Number of References: 40
Number of words in the Abstract: 233
Number of words in the Introduction: 741
Number of words in the Discussion: 1922

List of non-standard abbreviations: MD, molecular dynamics; NMR: nuclear magnetic resonance.

Molecular Pharmacology Fast Forward. Published on September 8, 2005 as DOI: 10.1124/mol.105.015685
This article has not been copyedited and formatted. The final version may differ from this version.

Abstract

Yondelis™ (trabectedin) is an antitumor ecteinascidin that binds covalently to the 2-amino group of the central guanine in the minor groove of selected DNA pyrimidine-G-G and purine-G-C triplets. Chromomycin A_3 is an aureolic acid derivative that binds non-covalently to the DNA minor groove in G/C-rich triplet sites as a metal-chelated dimer. Despite their different binding modes, the cytotoxicity profiles of these two drugs, as assessed in the COMPARE analysis carried out by the National Cancer Institute on data from 60 human tumor cell lines, are highly correlated (Pearson's correlation coefficient of 0.96). We now report that in a oligonucleotide containing the "natural bending element" TGGCCA, the structural distortions inflicted by the tail-to-tail bonding of two trabectedin molecules to adjacent target sites on opposing strands are strikingly similar to those observed in a crystal containing $d(TTGGCCAA)_2$ and two bound chromomycin A_3 molecules arranged in a head-to-tail orientation in the minor groove. In both complexes the double helix is characterized by being considerably unwound and possessing a notably widened minor groove. Binding of the drugs to this sequence could be favored by the distinct bends at each of the TpG steps that are already present in the free oligoucleotide. Simultaneous drug binding to the two strands in the manner described here is proposed to stabilize the helical structure of duplex DNA so as to prevent or hamper strand separation and stall replication and transcription forks.

Molecular Pharmacology Fast Forward. Published on September 8, 2005 as DOI: 10.1124/mol.105.015685
This article has not been copyedited and formatted. The final version may differ from this version.

Introduction

The potent anticancer agent Yondelis™ (trabectedin), presently in phase II/III clinical trials, was originally isolated with very low yields from the sea squirt *Ecteinascidia turbinata* (reviewed in Rinehart, 2000) but is now obtained in multigram quantities through chemical modification of microbially produced cyanosafracin B. Trabectedin consists of a polycyclic skeleton composed of three fused tetrahydroisoquinoline rings (Figure 1A) and binds to the minor groove of DNA by virtue of its reactive 21-carbinolamine group (reviewed in Gago and Hurley, 2002). The binding site covers three base pairs, and the exocyclic amino group of guanine is necessary for the covalent binding of the drug (Pommier et al., 1996). Sequence selectivity has been shown to operate predominantly through a set of well-defined hydrogen-bonding rules (Gago and Hurley, 2002) such that the preferred target triplets are 5'-RGC and 5'-YGG, where R and Y stand for purine and pyrimidine, respectively, and the underlined base is the guanine that undergoes alkylation by trabectedin. We have already reported on the remarkable similarity in the manner that trabectedin and zinc fingers from transcription factors such as EGR1/Zif268 or Sp1 (Marco et al., 2002) induce DNA structural distortions (Gago and Hurley, 2002), especially when three trabectedin molecules bind head-to-tail to three adjacent optimal binding sites on the same strand (Marco et al., 2002). In this case, trabectedin was shown to stabilize a DNA conformation that was intermediate between A- and B-form DNA (Ng et al., 2002).

Chromomycin A_3, on the other hand, belongs to the aureolic acid family of anticancer antibiotics isolated from *Streptomyces griseus* and consists of a planar heterocyclic aglycon connected to a disaccharide on one side and to a trisaccharide on the other

Molecular Pharmacology Fast Forward. Published on September 8, 2005 as DOI: 10.1124/mol.105.015685
This article has not been copyedited and formatted. The final version may differ from this version.

(Figure 1B). Chelation of two molecules by a single divalent metal ion, typically Mg^{2+}, leads to formation of a dimer that can bind to the DNA minor groove in G/C-rich sites that are at least 3 base pairs in length (Liu and Chen, 1994). Indeed, footprinting (Stankusm et al., 1992) and NMR spectroscopic (Gao and Patel, 1990) studies have shown strong, cooperative, and symmetrical binding of chromomycin A_3 dimers to adjacent TGG sequences on different strands (i.e., TGGCCA) when embedded in different self-complementary duplexes. The recent resolution by X-ray crystallography of the structure of an Mg^{2+}-chelated dimer in complex with a double-stranded $d(TTGGCCAA)_2$ octanucleotide (Protein Data Bank [PDB] accession code 1VAQ; http://www.rcsb.org/pdb/) has provided additional details about metal ion coordination and specific drug-DNA hydrogen bonds (Hou et al., 2004) In addition, this work has confirmed earlier evidence (Gao and Patel, 1990) that the DNA adopts a conformation that is best described by a combination of both B- and A-DNA structural parameters.

Interestingly, both trabectedin (NSC-648766) and chromomycin A_3 (NSC-58514) have been shown to exert at least part of their cytotoxicity by interfering with cell replication and transcription (Bonfanti et al., 1999; Chatterjee et al., 2001). Furthermore, comparison of the activity parameters for these two compounds on the panel of 60 human tumor cell lines of the National Cancer Institute (NCI) Anticancer Drug Screen (http://dtp.nci.nih.gov/docs/misc/common_files/ cell_list.html) has revealed a very high correlation coefficient (0.96) using the COMPARE algorithm (Paull et al., 1989). Thus, despite a very different mechanism of binding to DNA (i.e., covalent vs. non-covalent, carbinolamine activation vs. ion-mediated dimerization, etc), both drugs appear to be very similar in the way they induce apoptosis in different tumor

Molecular Pharmacology Fast Forward. Published on September 8, 2005 as DOI: 10.1124/mol.105.015685
This article has not been copyedited and formatted. The final version may differ from this version.

cell types. We reasoned that this might be due to the fact that the structural distortions they inflict on the DNA molecule are indeed comparable. To test this hypothesis, we have built and simulated using unrestrained molecular dynamics (MD) simulations in aqueous solution the structure of the self-complementary dodecanucleotide d(GTATGGCCATAC)$_2$ in a complex with two trabectedin molecules each covalently bonded to a different strand in a tail-to-tail fashion (Figure 2). For comparison and completeness, the same sequence has also been simulated under identical conditions in the absence of any bound drug. Thus, we have been able to assess the conformational preferences of the TGG triplet sequence, which is ubiquitously over-represented in human viral and eukaryotic sequences (Burge et al., 1992), including sites at or near replication origins of human mitochondrial DNA (Kang et al., 1997). Moreover, its complementary sequence is an important component of the so-called "CCAAT box" that is present in a high number of promoters (Mantovani, 1999), and the yuxtaposition of the two, i.e. TGGCCA, has been dubbed by some X-ray crystallographers as a "natural bending element" (Grzeskowiak et al., 1993).

Materials and Methods

Force Field and Charges. The second-generation AMBER force field (Cornell et al., 1995) was updated with new DNA parameters (Cheatham et al., 1999) for improved sugar pucker phases and helical repeat (parm98). Bonded parameters and quantum mechanically derived 6-31G*\\3-21G* RESP charges for guanine-bonded N12-protonated trabectedin have already been described (Marco et al., 2002).

Molecular Pharmacology Fast Forward. Published on September 8, 2005 as DOI: 10.1124/mol.105.015685
This article has not been copyedited and formatted. The final version may differ from this version.

Construction and Refinement of the Starting DNA Structures. A model of the free oligonucleotide was built using optimized parameters for B-DNA. The covalent complex between d(GTATGGCCATAC)$_2$ and trabectedin (one covalently modified guanine in the middle of each TGG triplet) was modeled using the same oligonucleotide in which the TGG triplet in each strand had been replaced by a TGG–trabectedin adduct as found in the energy-refined representative structure of the equilibrated (trabectedin)$_3$–d(GTGGCGGCGGCC)·d(GGCCGCCGCCAC) complex (PDB entry 1KML) reported earlier (Marco et al., 2002). The target TGGCCA was flanked by a 5'-TA-3' sequence on each side because both TpA and ApT steps are considered to be context-independent, and a terminal G:C pair at each end was used to prevent fraying. This initial geometry was then refined by means of 1000 steps of steepest descent energy minimization followed by 2000 steps of conjugate gradient energy minimization of only those atoms belonging to trabectedin and the replaced nucleobases. This procedure allowed readjustment of covalent bonds and van der Waals contacts without changing the overall conformation of the complex.

Molecular Dynamics of Free and Trabectedin–Bonded Oligonucleotides in Water. Each molecular system was neutralized by addition of the appropriate number of sodium ions, placed in positions of negative electrostatic potential, and immersed in a rectangular box of ~4600 TIP3P water molecules. Each water box extended 8 Å away from any solute atom, and the cutoff distance for the nonbonded interactions was 9 Å. Periodic boundary conditions were used and electrostatic interactions were represented using the smooth particle mesh Ewald method with a grid spacing of ~1 Å. The SHAKE algorithm was applied to all bonds involving hydrogens and an integration step of 2 fs

was used throughout. The simulation protocol for both the free dodecanucleotide and the covalent adduct was essentially as described (Marco et al., 2002) and made use of the SANDER module in AMBER version 6.0 (Case et al., 1999). Briefly, solvent molecules and counterions were relaxed by energy minimization and allowed to equilibrate during 50 ps of MD at 300 K and constant pressure around the atoms of the DNA or the drug-DNA complex, which were restrained to their initial positions with a harmonic restraint of 25 kcal mol^{-1} $Å^{-2}$. These restraints were gradually reduced in a series of successive minimizations, and the unrestrained system was then heated from 100 to 300 K during 10 ps followed by 0.5 ns of equilibration and 8.0 ns of data collection. System coordinates were saved every 2 ps for further analysis.

Analysis of the Molecular Dynamics Trajectories. Three-dimensional structures and trajectories were visually inspected using the computer graphics program PyMol (De Lano, 2004). Root-mean-square deviations (rmsd) from the initial or final structures and interatomic distances were monitored using the CARNAL module in AMBER. The conformational and helical parameters of the DNA dodecamers were analyzed by means of program CURVES (Lavery and Sklenar, 1988). The magnitude and directionality of the bending was related to the local helicoidal parameters roll and tilt, and quantified in terms of the angle of axis deflection (θ) and its orientation relative to the major groove (φ). Graphical display of these quantities for individual base pair steps was performed using polar plots that allow both the magnitude and the direction of the helical bend to be represented in the form of “bending dials” (Young et al., 1995), in which θ and φ are the radial and angular coordinates, respectively. Points on the northern hemisphere of the dial reflect positive roll and compression of the major

groove whereas bending into the minor groove is plotted on the southern hemisphere. Each ring on our bending dials indicates a 10º deflection of the helical axis, and φ runs clockwise from the top.

Solvent-Accessible Surface Area Calculations and Hydrophobic Effect. The reduction in DNA solvent-accessible surface area (SA) brought about by trabectedin binding was estimated as the difference between the total SA of the free DNA and the SA of DNA in the trabectedin–DNA complex using the program NACCESS (Hubbard and Thornton, 1993) and a water probe with a radius of 1.4 Å. The buried SA for trabectedin was likewise calculated as the difference in SA between twice the value of one isolated molecule and that of the two trabectedin molecules in the covalent complex. The hydrophobic effect involved was approximated by making use of the conversion factor of 20 cal·Å^{-2} obtained from a linear correlation between the SA of hydrophobic side chains in proteins and their free energy of transfer from a polar to a nonpolar solvent (Chothia, 1974).

All calculations were performed on the SGI R8000 Power Challenge at Alcalá University Computer Center, on the SGI R14000 Origin 3800 at CIEMAT (Madrid), and locally on SGI R5000 O2 workstations.

Results

General considerations. The low root-mean-square deviations (rmsd) of the coordinates of the free and drug-bonded oligonucleotides along the trajectory with respect to either the initial or the final structures and the absence of systematic drifting (see Figure S1 in Supplemental data) were indicative of adequate system equilibration

Molecular Pharmacology Fast Forward. Published on September 8, 2005 as DOI: 10.1124/mol.105.015685
This article has not been copyedited and formatted. The final version may differ from this version.

and strongly suggested that the simulations were long enough to sample the phase space and capture the inherent flexibility of this DNA molecule. All base pairs remained well stacked and internally hydrogen bonded, and no end-fraying was observed. In line with previous observations (Marco et al., 2002), bonding of trabectedin resulted in increased DNA stabilization as assessed by the smaller rmsd fluctuations in the simulation of the complex relative to the simulation of the free oligonucleotide.

An advantage of using a self-complementary DNA sequence is that the extent of sampling for each base-pair step is actually doubled because they are all represented twice. In addition, the similarity of the results for identical steps provides an indication of the consistency of the calculated structural parameters.

Description of the (trabectedin)$_2$–d(GTATGGCCATAC)$_2$ complex. The overall structure of the 2:1 complex is one in which each subunit A of trabectedin protrudes perpendicularly off the helix right in front of the guanine to which it is bonded (G5 and G17), the B subunits stack over the sugar rings of C20 and C8 in a manner reminiscent of that of typical nonintercalative minor groove binders, and the C subunits expose one flat side to the solvent whereas the other side makes extensive contacts with the sugar–phosphate backbone of the two nucleosides downstream of each covalently bonded guanine (Figure 3). Remarkably, whereas in the previous model with three trabectedin molecules bound “head-to-tail” to consecutive DNA triplets in the same strand no inter-drug contacts were apparent, in the present “tail-to-tail” arrangement both B subunits establish favorable van der Waals contacts at the junction of both DNA triplets. This may account for the negative roll detected at the G6/C7 junction, and also for the observation that the increase in positive roll at adjacent G/G steps (Table 1) is less than

Molecular Pharmacology Fast Forward. Published on September 8, 2005 as DOI: 10.1124/mol.105.015685
This article has not been copyedited and formatted. The final version may differ from this version.

that described in previously studied trabectedin-DNA (Gago and Hurley, 2002; Marco et al., 2002) and EGR1-DNA and Sp1-DNA complexes (Marco et al., 2003).

Monitoring the relative rotation of successive base pairs about an axis perpendicular to the plane of the base step along the trajectory showed the variation in helical twist angles among the different dinucleotide steps, which was averaged over time (Table 1). The greatest unwinding as a consequence of drug bonding takes place at T4/G5 and C8/A9 (=T16/G17) steps, which also show the largest values of roll angle (relative rotation of the base pairs about the long axis of the base step), in good accord with the known inverse relationship between this parameter and helical twist (Gorin et al., 1995). Both T4/G5 and C8/A9 steps appear in the predominant conformation CA+ (Table 1) that displays relatively small values of twist (~30^{o}) and positive roll. This twist-roll relationship is also valid for G6/C7 as this step displays both negative roll and the largest helical twist within the TGGCCA sequence.

Since roll and tilt components are known to contribute to bending of the double helix (Young et al., 1995), these values were calculated and displayed in the form of "bending dials" (Figure 4). Bending compressing the major groove, which arises from the positive roll reported in Table 1, is clearly apparent at T4/G5 and C8/A9 (=T16/G17) steps (dots plotted on the northern hemisphere of the dial) and of comparable magnitude in both despite the opposite tilt preferences. At T4/G5, the tilt component is negative (note the dots on the top left quadrant of the dial), indicative of bending into the phosphate backbone of its complementary Watson-Crick C20/A21 step. At C8/A9 the tilt component is positive but it would be negative if measured for the complementary T16/G17. Compression toward the minor groove is observed only at

Molecular Pharmacology Fast Forward. Published on September 8, 2005 as DOI: 10.1124/mol.105.015685
This article has not been copyedited and formatted. The final version may differ from this version.

the junction between the TGG triplets and is most likely a consequence of van der Waals interactions between subunits B of both drug molecules because this was not apparent in the simulation of the free DNA (see below).

The conformational features of the DNA in the (trabectedin)$_2$–d(GTATGGCCATAC)$_2$ complex are reminiscent of those previously found in the (trabectedin)$_3$–d(GTGGCGGCGGCC)·d(GGCCGCCGCCAC) complex and are best described as intermediate between those of A- and B-form DNA (Table 2). Average values for slide (relative translation of the base pairs about the long axis of the base step), twist, and minor groove width are closer to those of regular A-DNA. The negative sign of the X-displacement in both types of complex means that the base pairs have been displaced from the helical axis in the direction of the minor groove to create a deeper major groove, as found in A-DNA. With respect to sugar puckering and backbone conformation, three different situations are observed: (i) deoxyriboses with a C3'-endo conformation such as those attached to the cytosines (C8 and C20) that are complementary to the trabectedin–bonded guanines (G5 and G17); (ii) phase angles that oscillate during the trajectory from C3'-endo to O1'-endo conformations, as in C7, C19, T4 and T16, thus differing from the behavior expected for a regular B-DNA in which values are distributed between C2'-endo and C1'-exo; and (iii) deoxyriboses in C2'-endo with low standard deviation in their phase angles, as seen in those linked to the trabectedin–bonded guanines and the purines in the complementary strand (Table 3). These differences in phase angles appear to be correlated with distinct values in the glycosyl torsional angle, χ, such that nucleosides with high standard deviations in sugar puckering have average χ values midway between those corresponding to A-DNA (χ =

Molecular Pharmacology Fast Forward. Published on September 8, 2005 as DOI: 10.1124/mol.105.015685
This article has not been copyedited and formatted. The final version may differ from this version.

–154º) and B-DNA (χ = – 90º) whereas typical B-DNA values are found in nucleosides with low standard deviation in their phase angles. This effectively means that B-type nucleotides in the triplet region harboring the drug are paired with A/B-type nucleotides in the complementary strand. These altered sugar parameters correlate with the observed changes in slide and roll that are known to be necessary for the B$\rightarrow$A transition (Ng et al., 2000; Vargason et al., 2001).

Interactions between DNA and the two trabectedin molecules bonded in opposite strands. In the equilibrated complex of d(GTATGGCCATAC)· d(GTATGGCCATAC) with two trabectedin molecules covalently bonded to G4 and G17 (underlined), each drug is held in position by an intermolecular hydrogen bonding arrangement coincident with that originally proposed based on NMR experiments (reviewed in Gago and Hurley, 2002) and essentially identical to that found in other trabectedin–DNA complexes (Gago and Hurley, 2002; Marco et al., 2002): the protonated N12 of trabectedin is engaged in a hydrogen bond with the N3 acceptor atom of A21 in the first triplet and A9 in the second triplet; the methylendioxy oxygen facing the minor groove is involved in a hydrogen bond with the amino N2 of G5 and G17 (the bases following the guanines that are covalently modified by each trabectedin molecule), and the OH on subunit C is hydrogen bonded to the O1P of the phosphate linking C7-C8 and C19-C20 (Table 4).

Upon formation of the 2:1 trabectedin-DNA complex, the buried solvent-accessible surface areas of DNA and both trabectedin molecules are ~590 Å^2 and ~770 Å^2, respectively, of which ~185 Å^2 and ~340 Å^2 correspond to non-polar atoms. Thus, a substantial hydrophobic effect can be expected that would translate into an important

Molecular Pharmacology Fast Forward. Published on September 8, 2005 as DOI: 10.1124/mol.105.015685
This article has not been copyedited and formatted. The final version may differ from this version.

energetic contribution (~ 10.5 Kcal mol^{-1}) to the stabilization of the double helix.

Comparison of d(GTATGGCCATAC)$_2$ in the free state and with one trabectedin molecule bonded to each strand. The positioning of the bulky drug in the central region of the dodecanucleotide results in a notably wider minor groove at the TGGCCA sequence relative to the free DNA (Table 5). Similar results were found for the AGC-, TGG- and CGG-containing oligonucleotides reported previously (Gago and Hurley, 2002; Marco et al., 2002).

By comparing the average twist values for the different base steps in the trabectedin–DNA complex and in the free dodecanucleotide (Table 1), it can be noted that ApT and TpA steps retain their natural tendency to be underwound and overwound, respectively (Gorin et al., 1995), in both simulations. The most marked changes brought about by bonding of trabectedin, on the other hand, affect T4/G5, C7/C8, C8/A9 and A9/T10 steps, which not only are all unwound relative to the free DNA but also display much less fluctuation about their average values. This finding is in consonance with the enhanced DNA structural stabilization brought about by drug bonding discussed above (see Figure S1 in Supplemental data).

The reported differences in twist translate into similar differences in roll so that T4/G5 and C8/A9 steps appear bent toward the major groove (Figure 4). Even though T4/G5 and C8/A9 are shown to be intrinsically bent, greater bending is clearly observed upon trabectedin bonding, as demonstrated previously for an isolated triplet site (Gago and Hurley, 2002). Despite the relatively small increase in positive roll at G5/G6 and C7/C8 (=G17/G18), these steps show the largest negative slide (Table 1) that is associated with having trabectedin covalently bonded to G5 and G17, and this correlates with the

Molecular Pharmacology Fast Forward. Published on September 8, 2005 as DOI: 10.1124/mol.105.015685
This article has not been copyedited and formatted. The final version may differ from this version.

observed changes in minor groove width and glycosyl torsion angles (Tables 3 and 5).

Comparison with the (chromomycin A_3)$_2$–d(TTGGCCAA)$_2$ complex. Although two independent complexes in different packing environments are present in the asymmetric unit of the crystal lattice (Hou et al., 2004), they were found to be virtually superimposable (rms deviation of 1.24 Å over 983 atoms). Remarkably, this drug-DNA complex and the (trabectedin)$_2$–DNA complex that we have studied have several features in common such as:

- an unwound DNA and a considerably widened minor groove in the target TGGCCA region.

- a similar pattern of roll values: increased positive roll at TpG steps and small positive roll at GpG steps, together with negative roll at the central GpC step, which is more marked in the trabectedin-complex.

- negative slide at both GpG steps, in good agreement with the finding of χ values closer to those of A-DNA.

All of these characteristics describe a DNA conformation (Ng et al., 2000; Vargason et al, 2001) that is intermediate between those of A-DNA and B-DNA (Table 2). On the other hand, both drugs span a common triplet DNA site, and the O8 atoms of chromomycin A_3 are involved in similar hydrogen bonding interactions with the exocyclic amino group (N2) of G4 and G12 as those observed between the methylendioxy oxygens of trabectedin and the N2 of G5 and G19. The nonbonded equivalent of the covalent bond between the C21 of trabectedin and the N2 of G5 and G17 is the hydrogen bond that is established between the E-ring oxygen of chromomycin A_3 and the N2 of G3 and G11 (Figure 3).

Molecular Pharmacology Fast Forward. Published on September 8, 2005 as DOI: 10.1124/mol.105.015685
This article has not been copyedited and formatted. The final version may differ from this version.

Discussion

Unrestrained MD simulations have been instrumental for gaining further insight into the conformational subtleties that dictate sequence specificity and reactivity as well as into the structural basis of trabectedin-induced DNA bending and unwinding in the final covalent adducts. Although conformational details for DNA adducts containing trabectedin bonded to either a single site (Gago and Hurley, 2002) or three tandemly arranged triplet sites in the same DNA strand (Marco et al., 2002) have already been published, no structural information is available about the effects brought about by the drug when more than one molecule bind to closely spaced target sites on different strands. We now show that it is indeed feasible for two trabectedin molecules to bind in a tail-to-tail arrangement to two adjacent TGG sites placed on opposite strands.

Previous NMR-based MD simulations in aqueous solution of the covalent complexes between trabectedin and two non-self-complementary DNA nonanucleotides containing a central AGC or CGG triplet revealed that adduct formation brings about widening of the minor groove and restriction of some of the bending motions of free DNA (Gago and Hurley, 2002). These structural changes were shown to translate into significant bending of the DNA duplexes toward the major groove (PDB entries 1EZH and 1EZ5), mostly due to an increase in positive roll at the base pair step involved in covalent bond formation. Both the direction and magnitude of these bends were found to be in very good agreement with the macroscopic curvature detected in earlier electrophoretic gel migration and circularization experiments (Zewail-Foote and Hurley, 1999). Interestingly, when compared to their respective free DNA molecules, the CGG triplet

Molecular Pharmacology Fast Forward. Published on September 8, 2005 as DOI: 10.1124/mol.105.015685
This article has not been copyedited and formatted. The final version may differ from this version.

appeared to accommodate the drug with less distortion than AGC due to a slightly wider minor groove and both a decreased twist angle and a positive roll angle at the CpG step. This result suggested that the intrinsic bendability of a particular DNA sequence and its overall preorganization could facilitate specific recognition by trabectedin in much the same way as DNA sequence specificity for the minor groove covalent binders anthramycin and tomaymycin has been shown to correlate with the degree of bending and reaction kinetics (Kizu et al., 1993).

Model building based on this early work also suggested to us that tandem binding of several trabectedin molecules to suitable adjacent DNA sites was sterically and energetically feasible. Indeed, in agreement with the fact that both TGG and CGG triplets represent optimal binding sites for trabectedin (reviewed in Gago and Hurley, 2002), we were able to assess the stability of a (trabectedin)$_3$–d(GTGGCGGCGGCC)·d(GGCCGCCGCCAC) complex (PDB entry 1KML), demonstrating that the expected intermolecular hydrogen bonding scheme between each trabectedin molecule (covalently bonded to the underlined guanine) and each Y-G-G site was maintained along a nanosecond MD trajectory (Marco et al., 2002).

The present results now show for the first time that binding of two trabectedin molecules to target sites placed contiguously but on opposite strands is also feasible and leads to distinct structural distortions in the DNA oligonucleotide. Furthermore, the availability of the high-resolution (2.15 Å) structure of a Mg^{2+}-mediated chromomycin A_3 dimer bound to d(TTGGCCAA)$_2$ has allowed us to realize the striking similarity of the DNA structural parameters in both complexes (Table 2 and Figure 4). The rationale for performing such a comparison stemmed from the observation that trabectedin and

Molecular Pharmacology Fast Forward. Published on September 8, 2005 as DOI: 10.1124/mol.105.015685
This article has not been copyedited and formatted. The final version may differ from this version.

chromomycin A_3 induce highly correlated cytotoxic responses in the COMPARE analysis (r = 0.96). Remarkably, the overall structure that we find for the TGGCCA sequence in the complex of d(GTATGGCCATAC)$_2$ with two trabectedin molecules is virtually superimposable to the same sequence as found in a DNA octanucleotide containing two chromomycin A_3 molecules aligned in a head-to-tail orientation in the minor groove (rmsd of only 2.1 Å over phosphate backbone atoms and 3.1 Å over all non-hydrogen atoms of the common TGGCCA sequence). This structural similarity is presumably accompanied by increased duplex stabilization through interactions of each bound drug not only with both strands but also with the neighboring drug molecule. Given the amount of non-polar surface area that is buried upon complex formation (~525 Å^2), we would expect an important hydrophobic contribution not only to the free energy of trabectedin-DNA association but also to the ensuing stabilization of the double helix in the aqueous medium. For a complex of the type reported here it seems safe to assume that the increase in the temperature of DNA thermal denaturation will be larger than that obtained for a DNA oligonucleotide containing a single trabectedin adduct, which has been shown to be of 19^o for a 5'-AGC site (Zewail-Foote and Hurley, 2001a). Therefore, it is not unreasonable to think that the known ability of trabectedin to block the activity of exonuclease III (ExoIII) (Dziegielewska et al., 2004) or the helicase activities of both the SV40 large tumor antigen (T-antigen) (Zewail-Foote and Hurley, 2001a) and the UvrA$_2$B complex (Zewail-Foote and Hurley, 2001b) derives from this substantial stabilization which is likely to be amplified if two or more suitable triplets are tandemly or separately arranged in the oligonucleotide sequence.

To distinguish between drug-induced DNA distortions and sequence-dependent

Molecular Pharmacology Fast Forward. Published on September 8, 2005 as DOI: 10.1124/mol.105.015685
This article has not been copyedited and formatted. The final version may differ from this version.

intrinsic propensities, the dynamic behavior of the free d(GTATGGCCATAC)$_2$ oligonucleotide was simulated under identical conditions. Our results strongly suggest that this dodecamer shows two distinct bends produced by rolling at each TpG step (Figure 3) whereas no bending is apparent at the junction between TGG and CCA. These findings are in very good agreement with results from a two-dimensional NMR spectroscopy study reporting that GGC in the related self-complementary decamer d(CATGGCCATG)$_2$ forms a tight stack with parallel bases, and that high positive roll is present at both TpG steps (Dornberger et al., 1998). Nonetheless, they are at odds with earlier X-ray crystallography observations that stacked B-DNA double helices of general sequence C-C-A-x-x-x-x-T-G-G exhibited the same 23º bend across the -T-G-G C-C-A- nonbonded junction in the crystal lattice (Grzeskowiak et al., 1993) that was encountered in the middle of another decamer helix of sequence C-A-T-G-G-C-C-A-T-G (Goodsell et al., 1993). Because of this, the central DNA stretch studied in the present investigation, d(TGGCCA)$_2$, which can be simultaneously targeted by two molecules of either trabectedin or chromomycin A_3, was dubbed a "natural bending element" despite the fact that this curvature originated in crystal packing effects.

As reported earlier for complexes containing trabectedin bonded to a central guanine in AGC, CGG, or TGG triplets (Gago and Hurley, 2002; Marco et al., 2002), the minor groove in the present complex is notably wider than in the free oligonucleotide (Table 5), resulting in a compressed and deeper major groove in the central region where the drug is bound. This major groove compression is favored by the distinct behavior of pyrimidine/purine steps compared to purine/purine steps, which makes the former particularly susceptible to roll bending, as detected in experimental DNA structures

Molecular Pharmacology Fast Forward. Published on September 8, 2005 as DOI: 10.1124/mol.105.015685
This article has not been copyedited and formatted. The final version may differ from this version.

(Gorin et al., 1995). The preference of TpG/CpA for positive roll leads to decreased stacking interactions and this could offer an advantage for the binding of both proteins and drugs that induce or require this structural distorsion. In fact, this dinucleotide step is an important component of the CCAAT box, which is the core of the binding site for the evolutionary conserved transcription factor NF-Y (Mantovani, 1998). NF-Y makes important contacts with the minor groove and induces large directed bends, a capacity that is thought to be important for its promoter organizing activities. Interestingly, trabectedin, which can bind to the TGG triplet present in the complementary strand and also bends DNA (Zewail-Foote and Hurley, 1999), is able to abrogate the transcriptional activation of a number of genes that possess a CCAAT box in their regulatory regions, including *MDR1*, *c-JUN*, and *COL1A1* (Mantovani, 1998). Nevertheless, the effects of trabectedin are not exclusively related to NF-Y binding sites as this drug can also inhibit the trichostatin A-mediated transcriptional activation of the gene encoding $p21^{Cip1}$ (Friedman et al., 2002). Interestingly, the CCAAT-less $p21^{Cip1}$ promoter is regulated by major-groove binding of the zinc-finger-containing protein Sp1 to two or more of its G/C-rich motifs ("GC-boxes"), which also provide suitable triplet sites for trabectedin bonding in the minor groove (Gago and Hurley, 2002; Marco et al., 2002). In this regard, the recent finding that mithramycin A (a.k.a. plicamycin), a close analogue of chromomycin A_3, inhibits the transcriptional activation by Sp1 and p53 of the $p21^{Cip1}$ and *PUMA* (p53-upregulated mediator of apoptosis) gene promoters induced by 5-fluorouracil (Koutsodontis and Kardassis, 2004) can also be indicative of possible similarities in the mechanism of action of these two types of drugs. In addition, we note that transcription factors also bind to auxiliary

Molecular Pharmacology Fast Forward. Published on September 8, 2005 as DOI: 10.1124/mol.105.015685
This article has not been copyedited and formatted. The final version may differ from this version.

sequences adjacent to replication origins where they recruit chromatin remodeling factors that create either nucleosome-free regions or regions of specifically spaced nucleosomes (Melendy and Li, 2001). Remarkably, a very recent report has revealed strong inhibition, by nanomolar concentrations of trabectedin, of simian virus (SV40) DNA replication in BSC-1 green monkey kidney cells and HCT116 human colorectal carcinoma cells (Dziegielewska et al., 2004), together with accumulation of unusual DNA structures, which most likely suggests the existence of collapsed replication forks. In light of the results shown here and further work in progress (manuscript in preparation), it will be interesting to see to what extent binding of trabectedin can hamper assembly of the pre-replication complex and/or the helicase activity of its associated mini-chromosome maintenance (MCM) proteins (Lei et al., 2001). The extremely low concentrations of trabectedin and analogues that are necessary to cause cell cycle arrest and cell death (Rinehart, 2000) are suggestive of a trans-acting mechanism, most likely through one or more cellular DNA damage response pathways or checkpoints (Cox et al., 2000). This action would then be reminiscent of that evoked by adozelesin, another minor groove alkylator which, in contrast to trabectedin, binds selectively to AT-rich regions (Liu et al., 2000). In this respect, it is notable that cell sensitivity to trabectedin is somehow dependent on the presence of a proficient transcription-coupled pathway of nucleotide excision repair (Takebayashi et al., 2001; Damia et al., 2001; Erba et al., 2001).

In conclusion, the similarity in DNA structure between the $(\text{trabectedin})_2$–DNA complex studied herein and the recently reported $(\text{chromomycin } A_3)_2$–DNA crystal complex can be summarized by stating that both of them adopt characteristics

Molecular Pharmacology Fast Forward. Published on September 8, 2005 as DOI: 10.1124/mol.105.015685
This article has not been copyedited and formatted. The final version may differ from this version.

associated with A-DNA or DNA-RNA hybrids. The minor groove in TGG sequences provides a well-defined arrangement of hydrogen bonding donor and acceptor atoms that can interact with suitable functional groups present in these DNA-binding drugs but the intrinsic bendability of this sequence can also facilitate an indirect readout. Reaction of trabectedin with guanines embedded in suitable G/C-rich sequences (Friedman et al., 2002) could stabilize or prevent, depending on sequence context, the binding to DNA of transcription factors such as those belonging to the Sp1 family, which can behave as activators or repressors in the regulation of gene transcription. In this regard, it is of interest that inhibition of Sp1 DNA binding *in vivo* has recently been demonstrated for the mithramycin A (Koutsodontis and Kadarssis, 2000), a close analogue of chromomycin A_3. Also, the very high Pearson correlation coefficient ($r = 0.96$) obtained in the COMPARE analysis for chromomycin A_3 and trabectedin can be interpreted as indicative that both types of compounds may possess a similar mode of action (Paull et al., 1989). Hence, the structural similarities reported here provide a common foundation that can be of help in the elucidation of the molecular mechanism(s) involved. Among the logical experiments suggested by the present findings would be to compare the effects of these two drugs on gene transcription and to evaluate the possible dependence of chromomycin A_3's cytotoxicity on the integrity of the NER system.

Footnote. This study was supported by research grants (to F.G.) from the Spanish CICYT (SAF2003-7219-C02), PharmaMar (Colmenar Viejo, Madrid), and the National Foundation for Cancer Research. A fellowship to E. M. (Comunidad de Castilla-La

Molecular Pharmacology Fast Forward. Published on September 8, 2005 as DOI: 10.1124/mol.105.015685
This article has not been copyedited and formatted. The final version may differ from this version.

Mancha) is gratefully acknowledged. We thank the University of Alcalá Computing Center and the CIEMAT (Madrid) for generous allowances of computer time on their SGI servers.

Molecular Pharmacology Fast Forward. Published on September 8, 2005 as DOI: 10.1124/mol.105.015685
This article has not been copyedited and formatted. The final version may differ from this version.

References

Bianchi N, Osti F, Rutigliano C, Corradini FG, Borsetti E, Tomassetti M, Mischiati C, Feriotto G and Gambari R (1999) The DNA-binding drugs mithramycin and chromomycin are powerful inducers of erythroid differentiation of human K562 cells. *Br J Haematol* **104**:258–265.

Bonfanti M, La Valle E, Fernández-Sousa Faro JM, Faircloth G, Caretti G, Mantovani R and D'Incalci M (1999). Effect of ecteinascidin-743 on the interaction between DNA binding proteins and DNA. *Anticancer Drug Des* **14**: 179–186.

Case DA, Pearlman DA, Caldwell JW, Cheatham III TE, Ross WS, Simmerling CL, Darden TA, Merz KM, Stanton RV, Cheng AL, Vincent JJ, Crowley M, Tsui V, Radmer RJ, Duan Y, Pitera J, Massova I, Seibel GL, Singh UC, Weiner PK and Kollman PA. AMBER 6, University of California, San Francisco, 1999.

Chatterjee S, Zaman K, Ryu H, Conforto A and Ratan RR (2001) Sequence-selective DNA binding drugs mithramycin A and chromomycin A_3 are potent inhibitors of neuronal apoptosis induced by oxidative stress and DNA damage in cortical neurons. *Ann Neurol* **49**: 345–354.

Cheatham TE, Cieplak P and Kollman PA (1999) A modified version of the Cornell et al. force field with improved sugar pucker phases and helical repeat. *J Biomol Struct Dyn* **16**:845–862.

Chothia C (1974) Hydrophobic bonding and accessible surface area in proteins. *Nature* **248**:338–339.

Cornell WD, Cieplak P, Bayly CI, Gould IR, Merz KM, Ferguson DM, Spellmeyer DC, Fox T, Caldwell JW and Kollman PA (1995) A Second Generation Force Field for

the Simulation of Proteins, Nucleic Acids, and Organic Molecules. *J Am Chem Soc* **117**:5179–5197.

Cox MM, Goodman MF, Kreuzer KN, Sherratt DJ, Sandler SJ and Marians KJ (2000) The importance of repairing stalled replication forks. *Nature* **404**:37–41.

Damia G, Silvestri S, Carrassa L, Filiberti L, Faircloth GT, Liberi G, Foiani M and D'Incalci M (2001) Unique pattern of ET-743 activity in different cellular systems with defined deficiencies in DNA-repair pathways. *Int J Cancer* **92**:583–588.

De Lano W (2004) The PyMol molecular graphics system. De Lano Scientific LLC, San Carlos, CA, USA. http://www.pymol.org.

Dickerson RE (1993) Crystallographic analysis of C-C-A-A-G-C-T-T-G-G and its implications for bending in B-DNA. *Biochemistry* **32**:8923–8931.

Dornberger U, Flemming J and Fritzsche H (1998) Structure determination and analysis of helix parameters in the DNA decamer d(CATGGCCATG)$_2$ comparison of results from NMR and crystallography. *J Mol Biol* **284**:1453–1463.

Dziegielewska B, Kowalski D and Beerman TA (2004) SV40 DNA replication inhibition by the monofunctional DNA alkylator Et743. *Biochemistry* **43**:14228–14237.

Erba E, Bergamaschi D, Bassano L, Damia G, Ronzoni S, Faircloth GT, D'Incalci M. (2001) Ecteinascidin-743 (ET-743), a natural marine compound, with a unique mechanism of action. *Eur J Cancer* **37**:97–105.

Friedman D, Hu Z, Kolb EA, Gorfajn B and Scotto KW (2002) Ecteinascidin-743 inhibits activated but not constitutive transcription. *Cancer Res* **62**:3377–3381.

Gago F and Hurley LH (2002) Devising a structural basis for the potent cytotoxic

effects of ecteinascidin 743 (pp. 643-675), in *Small Molecule DNA and RNA Binders: From Synthesis to Nucleic Acid Complexes* (M Demeunynck, C Bailly & WD Wilson, Eds.) Wiley-VCH, Weinheim, Germany.

Gao XL and Patel DJ (1990) Chromomycin dimer-DNA oligomer complexes. Sequence selectivity and divalent cation specificity. *Biochemistry* **29**:10940–10956.

Goodsell DS, Kopka ML, Cascio D and Dickerson RE (1993) Crystal structure of CATGGCCATG and its implications for A-tract bending models. *Proc Natl Acad Sci USA* **90**:2930–2934.

Gorin AA, Zhurkin VB and Olson WK (1995) B-DNA twisting correlates with base-pair morphology. *J Mol Biol* **247**:34–48.

Grzeskowiak K, Goodsell DS, Kaczor-Grzeskowiak M, Cascio D and Dickerson RE (1993) Crystallographic analysis of C-C-A-A-G-C-T-T-G-G and its implications for bending in B-DNA. *Biochemistry* **32**:8923–8931.

Hou M-H, Robinson H, Gao Y-G and Wang AH-J (2004) Crystal structure of the [Mg^{2+}-(chromomycin $A_3)_2$]-d$(TTGGCCAA)_2$ complex reveals GGCC binding specificity of the drug dimer chelated by a metal ion. *Nucleic Acids Res* **32**:2214–2222.

Hubbard SJ, Thornton JM. NACCESS; Department of Biochemistry and Molecular Biology, University College London: London, 1993. http://wolf.bms.umist.ac.uk/naccess/

Kizu R, Draves PH and Hurley LH (1993) Correlation of DNA sequence specificity of anthramycin and tomaymycin with reaction kinetics and bending of DNA. *Biochemistry*, **32**:8712–8722.

Koutsodontis G and Kardassis D (2004) Inhibition of p53-mediated transcriptional responses by mithramycin A. *Oncogene* **23**:9190–9200.

Lavery R and Sklenar H (1988) The definition of generalized helicoidal parameters and of axis curvature for irregular nucleic acids. *J. Biomol. Struct. Dyn* **6**:63–91.

Lei M and Tye BK (2001) Initiating DNA synthesis: from recruiting to activating the MCM complex. *J Cell Sci* **114**:1447–1454.

Liu C and Chen FM (1994) Oligonucleotide studies of sequence-specific binding of chromomycin A_3 to DNA. *Biochemistry* **33**: 1419–1424.

Liu JS, Kuo SR, McHugh MM, Beerman TA and Melendy T (2000) Adozelesin triggers DNA damage response pathways and arrests SV40 DNA replication through replication protein A inactivation. *J Biol Chem* **275**:1391–1397.

Mantovani R (1998). A survey of 178 NF-Y binding CCAAT boxes. *Nucleic Acids Res* **26**:1135–1143.

Marco E, García-Nieto R and Gago F (2003) Assessment by molecular dynamics simulations of the structural determinants of DNA binding specificity for transcription factor Sp1. *J Mol Biol* **328**: 9–32.

Marco E, García-Nieto R, Mendieta J, Manzanares I, Cuevas C and Gago F (2002) A 3·(ET743)-DNA complex that both resembles an RNA-DNA hybrid and mimics zinc finger-induced DNA structural distortions. *J Med Chem* **45**:871–880.

Melendy T and Li R (2001) Chromatin remodeling and initiation of DNA replication. *Front Biosci* **6**, D1048-D1053.

Ng HL, Kopka ML and Dickerson RE (2000) The structure of a stable intermediate in the A$\leftrightarrow$B DNA helix transition. *Proc Natl Acad Sci USA* **97**: 2035–2039.

Paull KD, Shoemaker RH, Hodes L, Monks A, Scudiero DA, Rubinstein L, Plowman J and Boyd MR (1989) Display and analysis of patterns of differential activity of drugs against human tumor cell lines: development of mean graph and COMPARE algorithm. *J Natl Cancer Inst* **81:**1088–1092.

Pommier Y, Kohlhagen G, Bailly C, Waring M, Mazumder A and Kohn KW (1996). DNA sequence- and structure-selective alkylation of guanine N2 in the DNA minor groove by ecteinascidin 743, a potent antitumor compound from the Caribbean tunicate *Ecteinascidia turbinata. Biochemistry,* **35**:13303–13309.

Rinehart KL (2000) Antitumor compounds from tunicates. *Med Res Rev* **20**: 1–27.

Stankusm A, Goodisman J and Dabrowiak JC (1992) Quantitative footprinting analysis of the chromomycin A_3-DNA interaction. *Biochemistry* **31**:9310–9318.

Takebayashi Y, Pourquier P, Zimonjic DB, Nakayama K, Emmert S, Ueda T, Urasaki Y, Kanzaki A, Akiyama SI, Popescu N, Kraemer KH and Pommier Y (2001) Antiproliferative activity of ecteinascidin 743 is dependent upon transcription-coupled nucleotide-excision repair. *Nat Med*. **7**:961-6.

Vargason JM, Henderson K and Ho PS (2001) A crystallographic map of the transition from B-DNA to A-DNA. *Proc Natl Acad Sci USA*, **98**:7265–7270.

Young MA, Ravishanker G, Beveridge DL and Berman HM (1995) Analysis of local helix bending in crystal structures of DNA oligonucleotides and DNA-protein complexes. *Biophys J* **68**:2454–2468.

Zewail-Foote M and Hurley LH (1999). Ecteinascidin 743: a minor groove alkylator that bends DNA toward the major groove. *J Med Chem* **42**:2493–2497.

Zewail-Foote M and Hurley LH (2001a) Differential rates of reversibility of

ecteinascidin 743-DNA covalent adducts from different sequences lead to migration to favored bonding sites. *J Am Chem Soc* **123**:6485–6495.

Zewail-Foote M and Hurley LH (2001b) The inefficiency of incisions of ecteinascidin 743-DNA adducts by the UvrABC nuclease and the unique structural feature of the DNA adducts can be used to explain the repair-dependent toxicities of this antitumor agent. *Chem Biol* **8**:1033–1049.

Molecular Pharmacology Fast Forward. Published on September 8, 2005 as DOI: 10.1124/mol.105.015685
This article has not been copyedited and formatted. The final version may differ from this version.

Legends for figures

Fig. 1. Chemical structures of trabectedin (with three main subunits labeled A, B and C) and aureolic acid derivatives, chromomycin A_3 and mithramycin A (with sugar rings labeled A–E). Atom positions relevant to the text have been numbered.

Fig. 2. Schematic representation of the central region of the oligonucleotide studied showing sequence composition and numbering. The covalent bonds, as well as the hydrogen bonds (broken lines) between each trabectedin and the DNA are displayed.

Fig. 3. Polar plots ("bending dials") for all DNA internal steps in the $d(GTATGGCCATAC)_2$ oligonucleotide in (a) the absence and (b) the presence of two bonded trabectedin molecules. 2000 individual points are for structures separated by 2 ps throughout the course of the last 4 ns of the MD trajectory, and viewed together constitute a probability density. Bending compressing the major groove is plotted on the northern hemisphere of the dial. For comparison, bending dials have also been calculated for (c) the two independent $(chromomycin)_2$-$d(TTGGCCAA)_2$ complexes found in the 1VAQ crystal structure.

Molecular Pharmacology Fast Forward. Published on September 8, 2005 as DOI: 10.1124/mol.105.015685
This article has not been copyedited and formatted. The final version may differ from this version.

Fig. 4. Representative energy-refined average structure of the trabectedin-DNA complex (left) and the X-ray crystal structure of the $(chromomycin)_2$-DNA complex (PDB entry 1VAQ) (right). Trabectedin and chromomycin carbon atoms have been colored blue and orange, respectively. The Mg^{2+} ion and the two water molecules stabilizing the chromomycin dimer are shown as yellow and red spheres, respectively.

Table 1. Comparison of local helix parameters[a] for the base pair steps involved in binding of trabectedin (*top*) or chromomycin A_3 (*bottom*).

	Roll		Twist		Slide	
	Trabectedin (×2)	**Free**	**Trabectedin (×2)**	**Free**	**Trabectedin (×2)**	**Free**
T2-A3	9.1 (8.4)	4.4 (7.3)	37.3 (6.0)	39.6 (6.0)	-1.1 (0.6)	-0.3 (0.7)
A3-T4	-0.7(7.1)	1.1 (7.6)	30.3 (4.3)	30.0 (5.2)	-1.2 (0.4)	-0.9 (0.4)
T4-G5	15.3 (4.9)	7.6(8.3)	30.6 (4.4)	34.7 (7.2)	-0.4 (0.4)	-0.5 (0.7)
G5-G6	4.9 (7.9)	2.0 (5.3)	33.4 (4.8)	35.5 (5.0)	-1.4 (0.4)	-1.0 (0.7)
G6-C7	-7.0 (5.8)	0.1 (5.1)	34.3 (3.8)	35.1 (4.3)	-0.7 (0.4)	-1.3 (0.5)
C7-C8	5.8 (7.8)	3.3 (5.6)	33.2 (4.6)	32.7 (5.4)	-1.3 (0.5)	-1.6 (0.8)
C8-A9	12.2 (9.0)	8.9 (6.5)	30.8 (4.6)	39.5 (5.7)	-0.1 (0.5)	-0.5 (0.6)
A9-T10	2.1 (11.1)	4.5 (5.3)	23.1 (5.1)	25.2 (5.4)	-0.4 (0.5)	-0.8 (0.5)
T10-A11	9.1 (11.4)	4.5 (7.9)	39.9 (7.0)	41.1 (6.2)	-0.8 (0.7)	-0.6 (0.7)

	Roll	Twist	Slide
	chromomycin A_3 (×2)	**chromomycin A_3 (×2)**	**chromomycin A_3 (×2)**
T1-T2	8.7 (0.4)	35.8 (1.9)	–0.9 (0.2)
T2-G3	13.9 (4.5)	33.9 (5.2)	–0.8 (0.4)
G3-G4	0.4 (3.0)	22.3 (0.6)	–2.5 (0.1)
G4-C5	–1.2 (1.2)	29.9 (0.9)	–2.8 (0.1)
C5-C6	2.5 (1.5)	25.4 (4.3)	–2.3 (0.1)
C6-A7	14.5 (3.5)	32.4 (0.7)	–1.0 (0.3)
A7-T8	4.9 (0.3)	36.5 (0.2)	–0.6 (0.2)

[a] For the trabectedin complex, mean values and standard deviations (in brackets) were obtained from the last 4 ns of the MD simulations (2000 values). Minor losses of symmetry between A3-T4 and A9-T10 in this complex are accounted for by distortions in this latter step being induced by the presence of a "sticky" ion close to the sugar-phosphate backbone linking A9 and T10 (data not shown).
For the chromomycin A_3 complex, mean values and standard deviations were calculated from the two independent complexes present in the asymmetric unit of the crystal (Hou et al., 2004). Roll and twist angles are given in degrees, and slide is in Å.

Table 2. Conformational parameters of the TGGCCA DNA stretch in the (chromomycin $A_3)_2$:d(TTGGCCAA)$_2$ [a] and (trabectedin)$_2$–d(GTATGGCCATAC)$_2$ [b] complexes, in comparison to regular A-DNA and B-DNA.[c]

	A-DNA	ChromA_3-DNA	Trabectedin-DNA	B-DNA
Twist, degree	30.4	30.9	32.8	35.6
Roll, degree	10.0	5.9	6.1	1.6
X displacement, Å	–4.5	–2.2	–1.5	–0.1
Slide, Å	–1.7	–1.5	–0.5	0.4
Minor groove width, Å	10.0	9.5	9.0	6.2

[a] Measured and averaged for the TGGCCA sequence in the two X-ray crystal structures present in PDB entry 1VAQ.
[b] Energy-minimized average structure for TGGCCA obtained from the last 4 ns of the MD simulations.
[c] Mean values for A- and B-DNA from X-ray crystal structures (Ng et al., 2000)

Table 3. Comparison of phase and torsional angle χ in the d(GTATGGCCATAC)$_2$ dodecanucleotides studied.[a]

	Complex with two trabectedin molecules		Free	
	Phase(º)	χ (º)	Phase(º)	χ (º)
T4	102.7 ± 37.6	126.1 ± 18.1	124.8 ± 31.2	-110.3 ± 19.7
G5	159.1 ± 16.5	-104.8 ± 10.8	153.7 ± 19.8	-99.0 ± 16.3
G6	139.0 ± 17.5	-106.0 ± 11.8	156.3 ± 40.0	-119.1 ± 17.1
C7	97.0 ± 49.6	-136.8 ± 13.6	143.2 ± 26.5	-117.6 ± 15.9
C8	49.6 ± 76.4	-142.8 ± 9.8	132.6 ± 30.7	-123.9 ± 15.9
A9	181.4 ± 11.6	-106.1 ± 9.2	157.4 ± 35.8	-111.6 ± 14.6
T16	104.7 ± 34.7	-118.2 ± 23.5	133.9 ± 26.5	-99.3 ± 20.5
G17	162.6 ± 17.0	-106.6 ± 10.8	174.9 ± 51.4	-122.6 ± 25.6
G18	142.4 ± 14.5	-105.4 ± 11.2	141.9 ± 25.2	-120.8 ± 19.7
C19	126.5 ± 40.7	-129.6 ± 14.1	149.4 ± 23.9	-120.3 ± 13.2
C20	67.4 ± 78.2	-141.9 ± 11.5	130.9 ± 40.8	-122.4 ± 17.9
A21	174.8 ± 16.6	-104.5 ± 8.9	154.9 ± 29.0	-104.1 ± 17.6

[a] Averaged over the last 4 ns of the MD simulation.

Molecular Pharmacology Fast Forward. Published on September 8, 2005 as DOI: 10.1124/mol.105.015685
This article has not been copyedited and formatted. The final version may differ from this version.

Table 4. Intermolecular hydrogen bonding donor-acceptor distances (Å)[a] observed in the (trabectedin)$_2$–d(GTATGGCCATAC)$_2$ complex.[b]

	Mean distance	Standard deviation
N12-N3(A21)	3.0	0.2
N12-N3(A9)	3.0	0.2
OM-N2(G5)	3.1	0.1
OM-N2(G17)	3.1	0.1
OHC-O1P(G6)	3.1	0.1
OHC-O1P(G9)	2.8	0.5

[a] Averaged over the last 4 ns of the simulation
[b] OM and OHC are the methylenedioxy and phenolic oxygens from subunit C, respectively.

Table 5. Width of the minor groove[a] (Å) in the free d(GTATGGCCATAC)$_2$ dodecanucleotide, in the complex with two trabectedin molecules, and in the (chromomycin A$_3$)$_2$–d(TTGGCCAA)$_2$ complex.

	P5-P24	**P6-P23**	**P7-P22**	**P8-P21**	**P9-P20**	**P10-P19**	**P11-P18**	**P12-P17**
free	7.1 (1.5)	8.1 (1.4)	7.1 (1.7)	5.6 (1.7)	5.5 (1.3)	6.5 (1.6)	7.6 (1.5)	6.8 (1.5)
Trabectedin (×2) [b]	6.5 (1.5)	7.8 (0.8)	9.4 (0.4)	8.7 (0.6)	8.7 (0.6)	10.1 (0.5)	9.7 (1.5)	8.3 (1.6)

	P5-P16	**P6-P15**	**P7-P14**
chromomycin A$_3$ [c]	9.9	9.2	9.1

[a] Measured as the shortest inter-phosphate distances across the groove (P-P distance minus 5.8 Å). The P-P distance in regular B-DNA is 5.9 Å. Measurement of O1'-O1' distances provides similar relative differences.
[b] Mean values obtained from the 4 ns of the MD simulations are shown, with standard deviations in brackets.
[c] Measured and averaged for the TGGCCA sequence in the two X-ray crystal structures present in PDB entry 1VAQ.

Molecular Pharmacology Fast Forward. Published on September 8, 2005 as DOI: 10.1124/mol.105.015685
This article has not been copyedited and formatted. The final version may differ from this version.

1

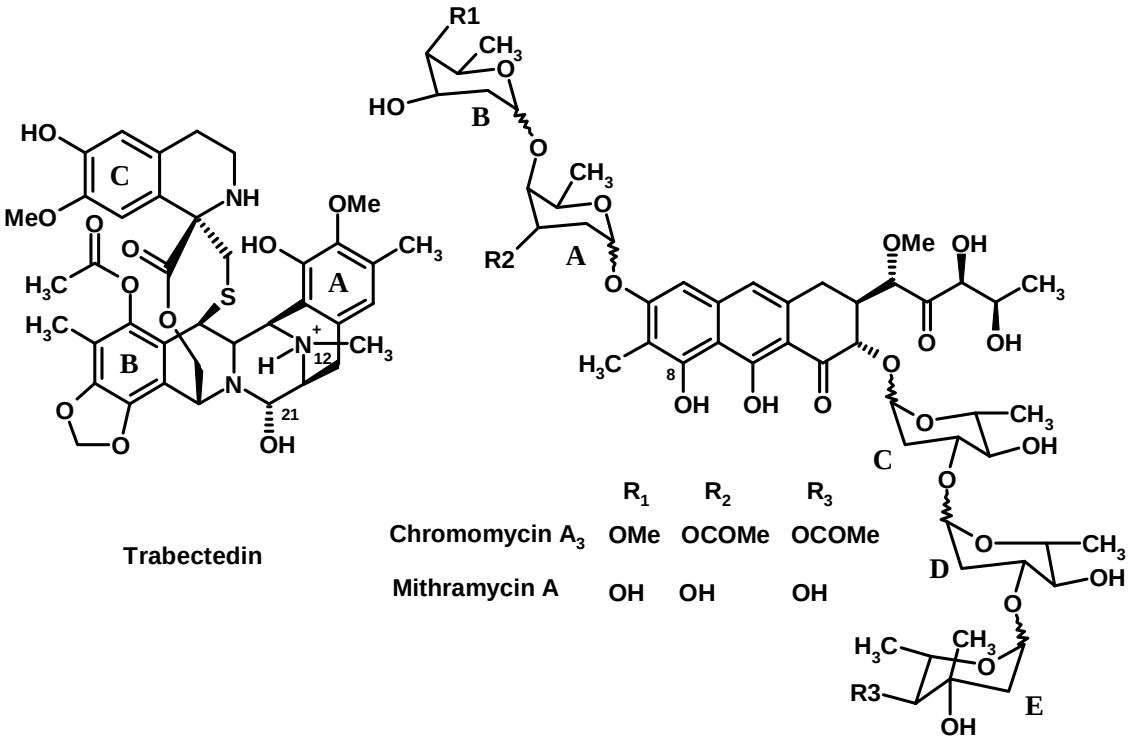

	R_1	R_2	R_3
Chromomycin A_3	OMe	OCOMe	OCOMe
Mithramycin A	OH	OH	OH

Trabectedin

Molecular Pharmacology Fast Forward. Published on September 8, 2005 as DOI: 10.1124/mol.105.015685
This article has not been copyedited and formatted. The final version may differ from this version.

2

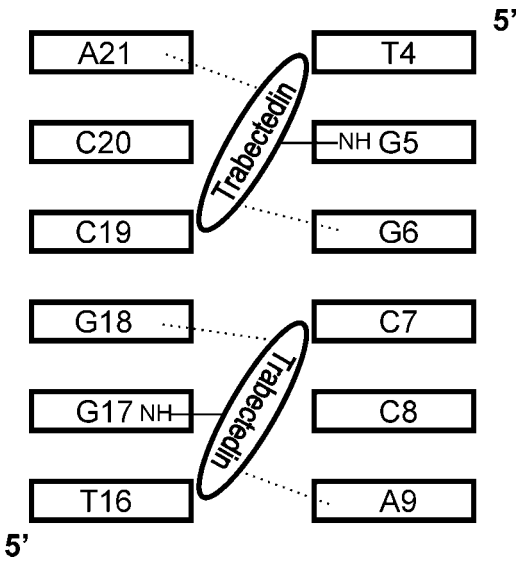

Molecular Pharmacology Fast Forward. Published on September 8, 2005 as DOI: 10.1124/mol.105.015685
This article has not been copyedited and formatted. The final version may differ from this version.

3

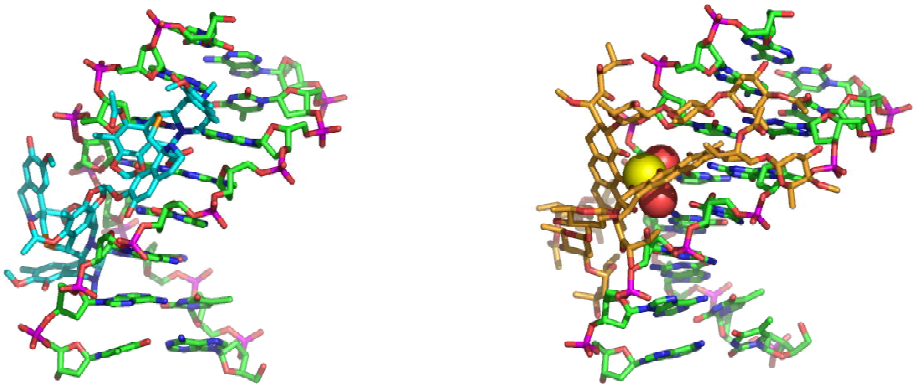

Molecular Pharmacology Fast Forward. Published on September 8, 2005 as DOI: 10.1124/mol.105.015685
This article has not been copyedited and formatted. The final version may differ from this version.

4